

Electrochemical Performances of SOFC as Function of the Sputtered Parameters of the YSZ Electrolyte

P. Briois^{a, b}, J. H. Park^c, A. Billard^{a, b}, and J.W. Son^c

^aFEMTO-ST Institute (UMR CNRS 6174), Univ. Bourgogne Franche-Comté, UTBM,
2 Place Lucien Tharradin, F-25200 Montbéliard Cedex, France

^bFR FCLab 3539, 90000 Belfort

^cCenter for Energy Materials Research, Clean Energy Institute, Korea Institute of Science and Technology (KIST), Korea

Yttria Stabilized Zirconia (YSZ) coatings were synthesized by reactive magnetron sputtering under different bias powers applied to the substrate holder and different thickness. All as-deposited coating presents a face centered cubic (f.c.c) structure of zirconia with dense and adhesive morphology. All coatings are adherent and the density increase with the bias power applied on the porte substrate holder. The best performance of the cell obtain in this study is 1060 mW.cm^{-2} at 650°C when the electrolyte thickness is $1.8 \mu\text{m}$.

Introduction

Due to global warming, the depletion of fossil fuels and the growing demand for energy from the population, it seems necessary to develop clean, efficient and environmentally friendly technique to produce electricity (1-3). Solid Oxide Fuel Cell (SOFC) are one of the ways to meet this challenge because of their performance, their impact on the environment and the possibility to use a various fuel (1,3-4). To consider a mass development of SOFC, it is necessary to reduce their operating temperature (3). Indeed, a high operating temperature makes it possible to obtain good electrochemical performances, but this is done to reduce the lifetime of the cells (5). The reduction of the operating temperature without loss of electrochemical performance requires the development of SOFC thin film by the use of surface treatment techniques and reduce the temperature fabrication (6-7). The required properties of an SOFC electrolyte are a good ionic conductivity of oxygen and no electrical conductivity, fine to limit the ohmic drop of the cell to reduce the temperature of use, dense to be gas-tight as well good chemical and thermomechanical compatibility with electrode materials (2,5).

The anode support cell developed in this work implements conventional SOFC materials namely: a Ni-YSZ cermet for the anode, a YSZ electrolyte, a GDC buffer layer and an LSCF cathode (3). The buffer layer in GDC is used in order to reduce the reactivity between the cathode and the electrolyte which leads to performance falls by the appearance of pyrochlore phase at the electrolyte / cathode interface (8). The technique used is magnetron sputtering because of its environmental friendliness and the fact that it is suitable for thin, dense and complex composition film synthesis (7). The work of J. A. Thornton (9), completed by A. Anders (10), , shows that the densification of a PVD film is obtained when the energy of the plasma species is important, therefore during a low

working pressure during the deposition phase as well as the application of a polarization at the sample holder. This study focuses on the importance of electrolyte synthesis parameters on cell performance, in particular on the polarization power of the sample holder as well as on the thickness of the film. YSZ layers are developed under reactive conditions from a metal target.

Experimental details

Elaboration of the SOFC

Anode layer: A 2 cm by 2 cm and 1-mm-thick NiO–YSZ (NiO/8YSZ = 56:44 wt%) anode support was fabricated by tape casting. 150- μ m-thick NiO–YSZ tapes with poly(methyl methacrylate) (PMMA) as a pore-forming agent and 30- μ m-thick NiO–YSZ tapes without PMMA were also fabricated by tape casting. Then, seven layers of the 150- μ m-thick tape and one layer of the 30- μ m-thick tape were laminated at 75°C under a uniaxial pressure of 15 MPa. The laminated substrate was sintered at 1300°C for 4 h to fabricate a completely rigid substrate. For more details see our previous work (11).

Electrolyte layer: The experimental device is a 100-litre Alcatel SCM 650 sputtering chamber pumped down via a system combining XDS35i Dry Pump and a 5401CP turbo-molecular pump. The sputtering chamber is equipped with three 200 mm diameter magnetron targets and with a 620 mm diameter rotating substrate holder parallel to the targets at a distance of about 110 mm. The distance between the targets axis and that of the substrate holder is 170 mm. The Zr-16 at.% Y target is supplied thanks to a pulsed DC Advanced Energy dual generator allowing the control of the discharge current, power or voltage. In the present study, the discharge current is fixed at 2.5 A. The substrates are alumina pellets, glass slides as well as anode substrate positioned next to the target at 170 mm from the axis of the substrate holder. Argon and oxygen flow rates are controlled with MKS flowmeters and the pressure is measured using a MKS Baratron gauge. The deposition stage is monitored using a closed loop control PEM (Plasma Emission Monitoring) system using optical emission spectroscopy (OES). The technique is based on the measurement of the optical intensity of the zirconium emission line (360.12 nm) measured on the area close up to the target. The signal is sent via an optical fibre to a Ropper Scientific SpectraPro 500i spectrometer, with a 1200 groove mm⁻² grating and a photomultiplier tube (Hamamatsu R 636). Then, the information is transferred to a computer where a program developed under Labview® monitors the oxygen flow rate to maintain the selected intensity of the optical signal of the zirconium line. For more details concerning the plasma emission monitoring techniques you can see our previous work on the elaboration of the electrolyte (12-13) and cathode material for SOFC (14).

Buffer layer: A 200-nm-thick gadolinia-doped ceria (GDC) buffer layers were deposited using PLD at a substrate temperature of 700°C and a Pamb of 6.67 Pa (11).

Cathode layer: A 3- μ m-thick lanthanum strontium cobaltite (LSC) layer with a 1 cm \times 1 cm area was deposited onto the GDC by PLD at room temperature and a Pamb of 13.3 Pa, followed by post-annealing at 650°C in air for 1 h to crystallize the cathode (11).

Structural and Morphological Characterization

The coatings morphology is characterized by Scanning Electron Microscopy (SEM) using a JEOL JSM 7800 F. The structural features of the coatings are identified in Bragg Brentano configuration X-ray diffraction using a BRUKER D8 focus diffractometer (CoK α 1+ α 2 radiations) equipped with the LynxEye linear detector. X-Ray Diffraction (XRD) patterns are collected at room temperature during 10 min in the [20°-80°] scattering angle range by a step of 0.019°. The coating thickness is determined using the “step” method (a small surface of the substrate is covered with a tape that is removed after deposition leaving a step due to the coating thickness) with an Altysurf profilometer from Altimet allowing an accuracy of about 20 nm. Before each measurement, the calibration of the experimental device was realized with a reference sample number 787569 accredited by CETIM, France.

Electrical Measurements

Air and humidified H₂ (3% H₂O) were used as the oxidant and fuel, respectively. The cell operating temperature varied from 650 to 450°C at intervals of 50°C, and the electrochemical impedance spectra (EIS) and current–voltage–power (I–V–P) curves were obtained at each temperature. Each EIS was observed over a frequency range of 105 Hz to 10⁻¹ Hz. The AC amplitude of the impedance measurements was 50 mV. An Iviumstat electrochemical analyzer (Iviumstat, Ivium Technologies) was used to obtain these EIS and I–V–P curves.

Result and Discussion

First Study

The sputtering parameter for producing the YSZ layer are summarized in Table I. Under the operating conditions, the deposition rate is 750 nm.h⁻¹, which is much greater without PEM system (13).

Table I. Sputtering parameter.

Target (at.%)	Intensity (A/kHz)	Rf bias power (W)	Ar flow rate (sccm)	O ₂ Flow rate (sccm)	Set Point PEM (%)	Total pressure (Pa)
Zr-16Y	2.5/50	20	20	adjust	35	0.2

Figure. 1 reveals that the film is crystallized under the cubic face-centered structure of the zirconia as-deposited and after a annealing treatment of 2 hours in air at 500°C. NiO diffraction peaks from the substrate are also observed. The annealing treatment leads to a displacement of the diffraction peaks to the right which reflects an evolution of the lattice parameter from 0.51411 nm to 0.51321 nm respectively for the as-deposited and annealed film. In agreement with JCPDS 30-4068 which gives a lattice parameter of 0.5139 nm, the as-deposited film is under extension constraints whereas after annealing it is under compression constraints. The appearance of stress during the deposition phase is induced by the application of the 20 W polarization at the porte substrate holder, and the modification of the nature of the stresses within the film during the heat treatment is due to the fact that the as-deposited coating is not saturated in

oxygen (11). This oxygen deficiency is compensated during heat treatment under static air. The SEM observation of the fracture facies of the rough film shows good adhesion with quality interfaces (Figure 2a). The YSZ layer has a slightly columnar appearance that is typical of a PVD film. After the annealing treatment in static air for 2 hours at 500°C, the film is still adherent and denser (FIG. 2b) which reinforces the observations of the XRD measurement.

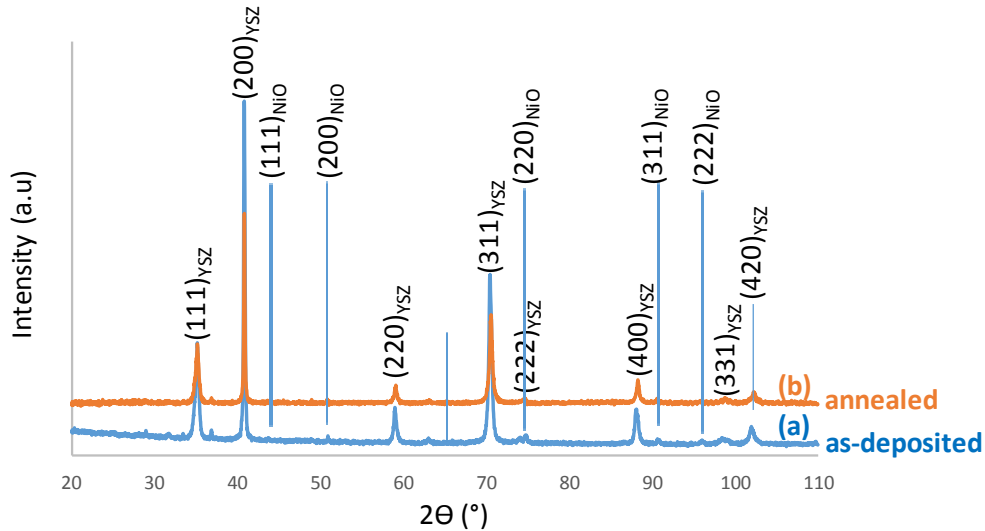


Figure 1. XRD measurements of (a) as-deposited YSZ coatings and (b) after annealing during 2 h under static air (orange).

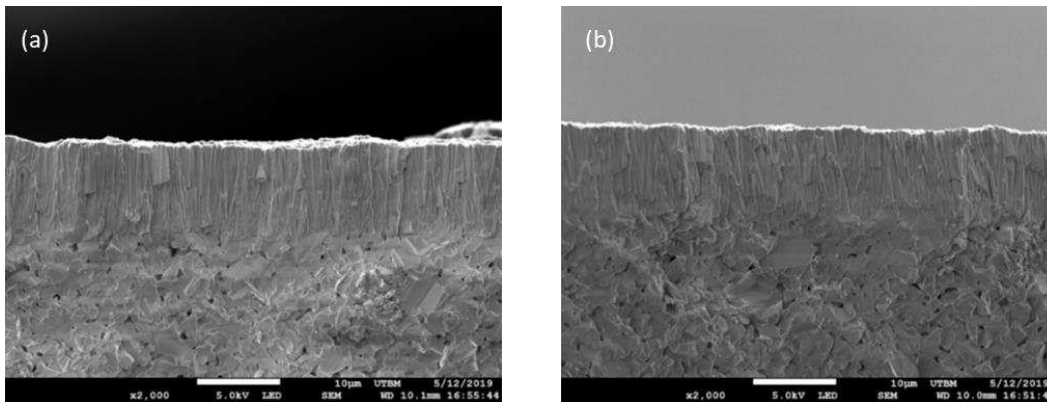


Figure 2. SEM view of brittle fracture cross section of (a) as-deposited and (b) annealed samples.

Figure 3 shows the electrochemical performances of the cell for each temperature with figure 3a and 3b which respectively represent the I-V-P measurements and the Nyquist diagram for each temperature. Table II is obtained from these measurements in which a comparison of the performances of the cell with the theoretical magnitude for each temperature is shown. Before the measurement, the anode was reduced during 10 h at 600°C and the measurements were recorded during decreasing temperature every 50°C from 600 to 450°C, then raised to 650°C. The value of the OCV is lower than the calculated theoretical value, respectively 1.038V and 1.122 V because of a problem of sealing of the YSZ layer. This problem of tightness of the electrolyte is caused by the too

columnar appearance of the layer. In addition, the ASR of the cell obtained is greater than the theoretical value for all the temperatures. The increase in ASR results from the fact that the ionic conductivity of the YSZ film is lower than the conductivity of the bulk YSZ (16). The observation of the brittle cross section of the cell (figure 3c) as well as the cathode surface (figure 3d) after the electrochemical measurements reveal the good behavior of each layers as well as the integrity of the cell.

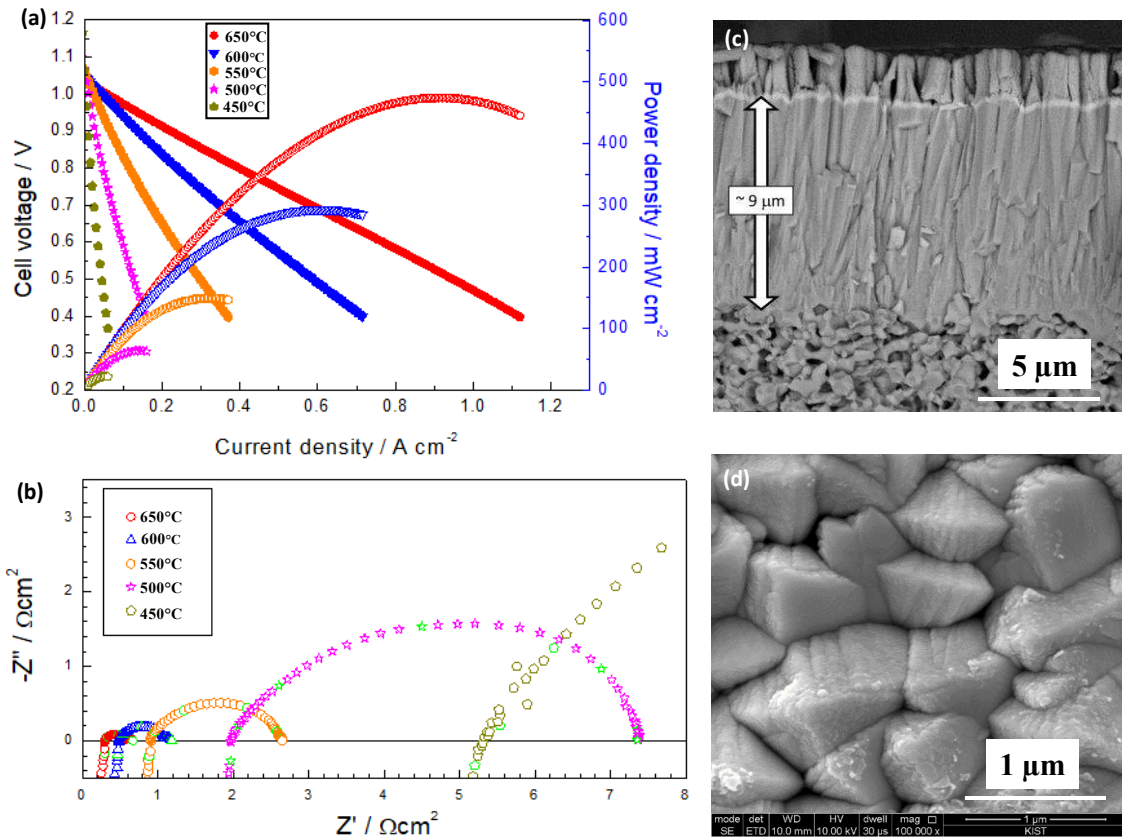


Figure 3. (a) Potential and Power versus Current of complete cell and (b) Nyquist diagram for different temperature. (c) SEM view of surface of cathode side and (d) brittle fracture cross section of complete cell after electrical measurement.

Table II. electrical measurements data vs thermodynamics calculus.

T (°C)	OCV (V)	Ideal OCV (V)	Ohm. ASR at OCV ($\Omega\text{-cm}^2$)	ASR of ideal 10 μm YSZ ($\Omega\text{-cm}^2$)	Pol. ASR at OCV ($\Omega\text{-cm}^2$)	Power Density at 0.7V (mW/cm^2)	Peak Power Density (mW/cm^2)
600	1.051	1.13	0.481	0.226	0.706	220.1	293.6
550	1.061	1.14	0.900	0.502	1.749	108.2	149.5
500	1.067	1.148	1.960	1.238	5.395	44.7	64.0
450	1.065	1.157	5.330	3.858	18.283	17.3	22.5
650	1.038	1.122	0.296	0.111	0.372	369.8	474.4

Second Study

During this second series of experiments, we had to define new deposition parameters to increase the density of the films in order to produce films with different thicknesses from 2 to 14 μm . One of the possible parameters is to modify the power applied on the sample holder in order to increase the energy of incident species on the substrate holder. To do this, we used the results of a previous study conducted on gadolinia doped ceria coatings (GDC) (17), we observed that the power applied increase on the sample holder allows to densify the coating but from certain value (80W) it appears that films no adherent. This adhesion problem is mainly related to the presence of stress in the film, they relax during it cracking and / or its desquamation. The constraints are even more important that the atoms constituting the film are big and heavy, in our previous study the film of GDC is composed of Ce, Gd and O which are larger, and heavier than the elements Zr, Y and O from the YSZ for this study. We also had to minimize the constraints in the YSZ film because our goal was to make a fairly thick 14 μm film. The deposit conditions are reported in Table III, line 1.

Table III. Sputtering parameter for the second study.

Target (at.%)	Intensity (A/kHz)	Rf bias power (W)	Ar flow rate (sccm)	O ₂ Flow rate (sccm)	Set Point PEM (%)	Total pressure (Pa)
Zr-16Y	2.5/50	0 to 80	10	adjust	30	0.1
		80	15		45	0.15

As shown in figure 4, the increase of the polarization power makes it possible to densify the film and they are all adherent after an annealing of 2 hours in air at 500°C. We have not tried to put a bias voltage higher than 80 W for the reasons mentioned above. We have reduced the working pressure to 0.15 Pa which is lower than the first series (0.2Pa) because in agreement with the work of A. Anders (10), the reduction of the working pressure makes it possible to densify the film. However, when observing the effect of the polarization power on the porte substrate holder a working pressure of 0.1 Pa, but for such pressure the amount of gas is too low which leads to instability of the discharge. Such instability is not compatible with our goal of making a thick film of several micrometers. In addition, the set point has been increased to increase the oxygen deficiency of the film during processing which will lead to greater volume expansion during the annealing phase (13). Zirconia is a material that is transparent when it is saturated with oxygen. The measurement of the transmittance of the films produced under different set point shows that the films are more and more absorbent with the increase in the regulation set point, and thus with the oxygen deficiency. However, there is a compromise in the synthesis between putting enough oxygen to prevent cracking of the film during its crystallization and add a limited amount to allow a volume expansion during the heat treatment to densify the material and fill the gaps pores of the anode.

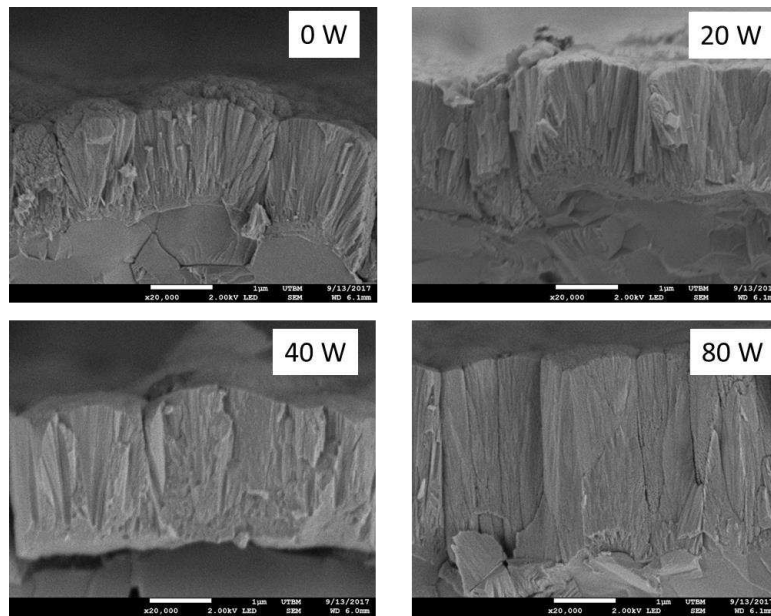


Figure 4. SEM view of brittle fracture cross section of YSZ coatings annealed 2 h at 500°C under static air on anode substrate with different bias powers.

The operating conditions are summarized in Table III, line2. In these condition, the deposition rate is of the order 1200 to 1500 $\text{nm}\cdot\text{h}^{-1}$ which is about twice as large as in the first series and in agreement with our previous work it is approximately 7 times higher in the absence of the use of the PEM system (13). This higher sputtering rate is directly related to the modification of the set point value which makes the film more oxygen deficient compared to the first series. In magnetron sputtering the deposition rate of a metal is much greater than that of a ceramic compound (18). The operating conditions allowing the synthesis of a denser film being now defined, it will be sufficient to modify the deposition time to obtain the thickness of the desired film on the anode made according to the same protocol as the series 1. All the films are crystallized under the cubic face-centered structure of the zirconia and the heat treatment makes it possible to increase the crystallization as well as to relax the stresses. Brittle cross section observation by SEM of the cells after the electrochemical test reveals clear interfaces, as well as a dense electrolyte (figure 5). Moreover, it appears that the electrolyte doesn't have a columnar appearance as in the first measurement series (figure 3) and that the modification of the synthesis parameters made it possible to densify the YSZ layer.

This observation is confirmed by the determination of complete cell performance (figure 6). Indeed, the OCV obtained for the thinnest film (1.8 μm) is almost equivalent to that of the first series which has a thickness approximately 5 times greater (Table IV). The performance of the cell increases with the reduction of the electrolyte which agrees with the literature (6). The maximum power is obtained from 1060 $\text{mW}\cdot\text{cm}^{-2}$ at 650°C for the cell having an electrolyte of 1.8 μm . The modification of the experimental parameters allowed to increase the performances of the cell because of the increased density of YSZ films.

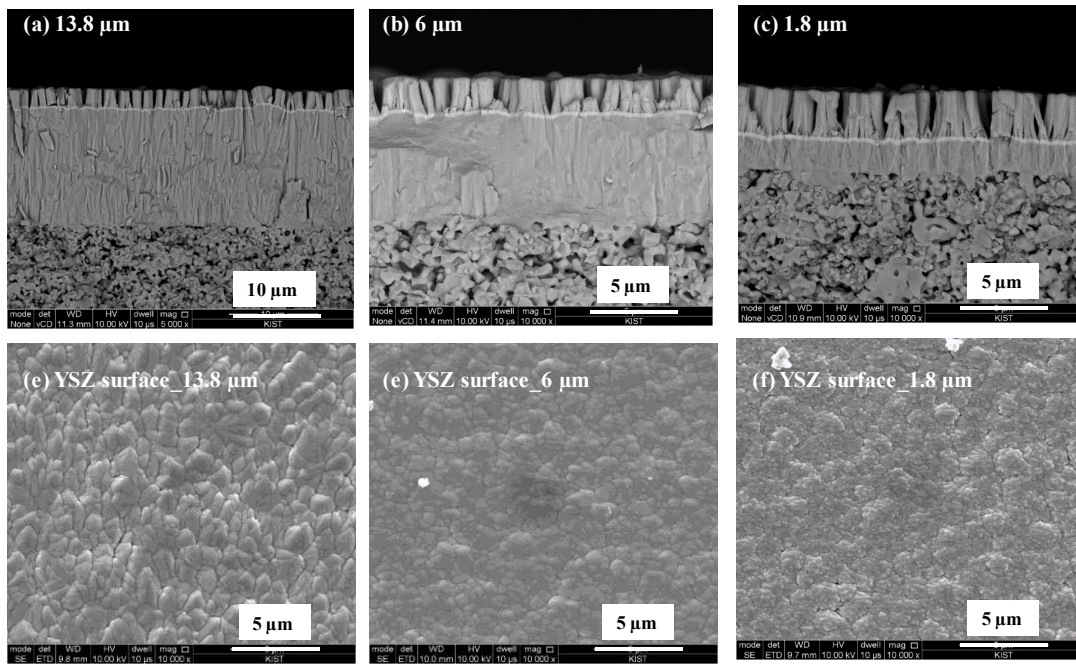


Figure 5. (a, b, c) SEM view of brittle fracture cross section of complete cell with different YSZ thicknesses after electrochemical measurements and (d, e, f) SEM view of the surface of YSZ coating after annealing.

Table IV. Electrical measurements data of complete cell with different electrolyte thicknesses for two temperature.

Temperature (°C)	Thickness (μm/study)	OCV (V)	Ohm. ASR at OCV ($\Omega\text{-cm}^2$)	Pol. ASR at OCV ($\Omega\text{-cm}^2$)	Power Density at 0.7V (mW/cm^2)	Peak Power Density (mW/cm^2)
500	1.8 (2)	1.066	0.637	3.159	100.1	157.1
	6 (2)	1.147	3.339	4.750	47.1	54.8
	9 (1)	1.067	1.960	5.395	44.7	64.0
	13.8 (2)	1.127	4.030	4.610	40.0	46.4
650	1.8 (2)	1.034	0.076	0.292	801.5	1060.5
	6 (2)	1.123	0.284	0.636	508.6	648.6
	9 (1)	1.038	0.234	0.372	369.8	474.5
	13.8 (2)	1.114	0.359	0.609	434.6	549.3

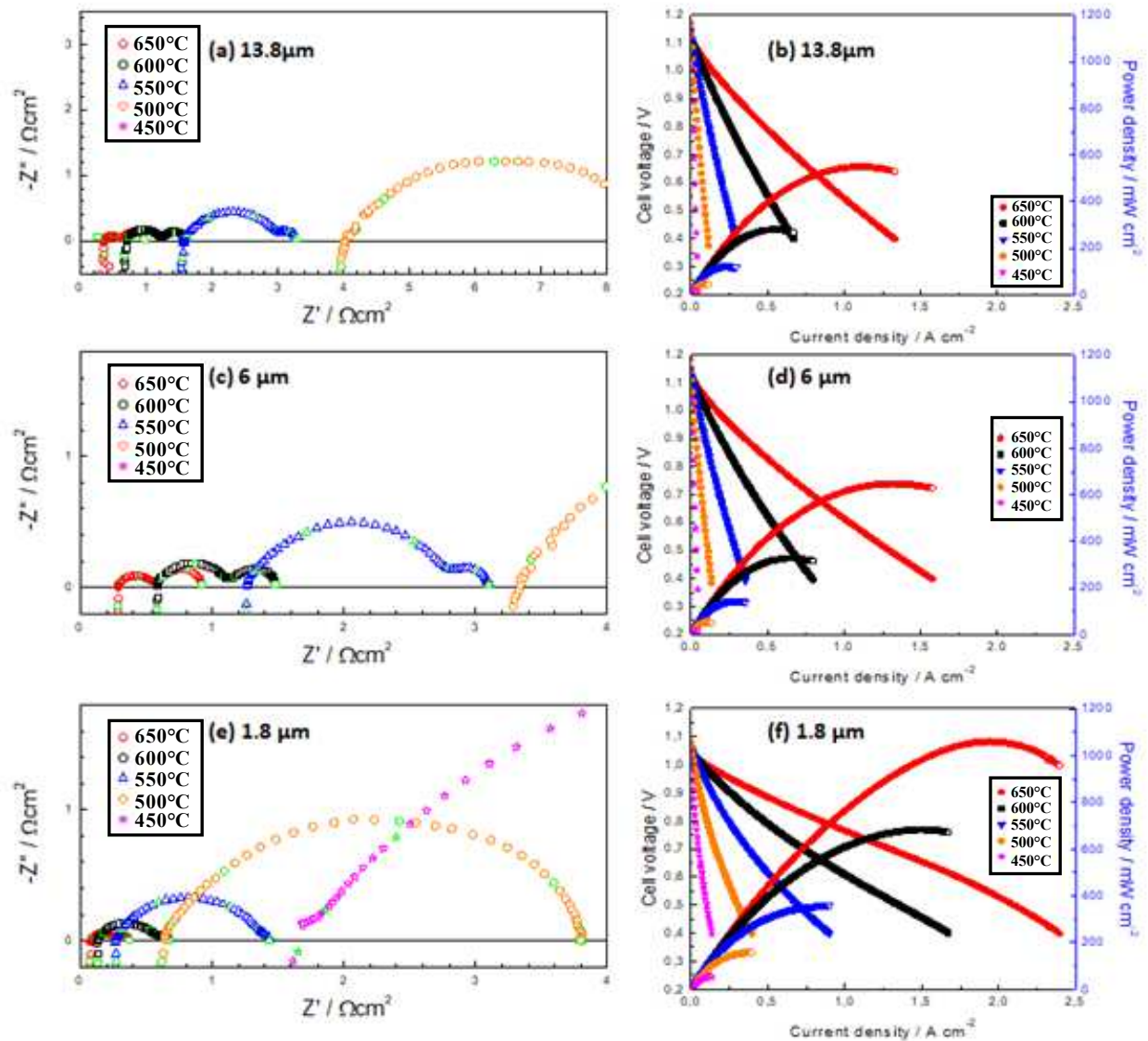


Figure 6. (a, c, e) Nyquist diagram and (b, d, f) Potential and Power versus Current of complete cell for different temperature and different YSZ electrolyte thicknesses.

Conclusion

In this work, the influence of bias power applied to the substrate holder and the thickness of YSZ coatings deposited by reactive magnetron sputtering has been studied. The application of PEM system could allow to obtain a relatively high sputtering rate, up to seven times higher than without PEM system. It should be noted that the density of the YSZ increase with the bias power applied on the substrate and annealing treatment relax stresses appears during the elaboration and increase the oxygen content into the coating. All coatings present f.c.c structure of zirconia before and after thermal treatment. SEM observation of the brittle cross section of the cells after the test shows the good quality of all the layers as well as the interfaces of the unit cell. The performance of the cell

increases with the decrease of the thickness of the electrolyte (1060 mW.cm⁻² at 650°C then the thickness is 1.8 µm)

Acknowledgments

This study was granted by the Pays de Montbéliard Agglomeration.

References

1. A. Boudghene Stambouli and E. Traversa, *Renewable and Sustainable Energy Review*, **6**, 433 (2002).
2. S.M. Haile, *Acta materialia*, **51**, 5981 (2003).
3. M. Liu, M. E. Lynch, K. Blinn, F. M. Alamgir and Y.M. Choi, *Materials Today*, **14**, 534 (2011).
4. S.P.S. Badwal and K. Foger, *Ceramics International*, **22**, 257 (1996).
5. A. Weber and E. Ivers-Tiffée, *Journal of Power Sources*, **127**, 273 (2004).
6. A.J. McEvoy, *Solid State Ionics*, **132**, 159 (2000).
7. L.R. Pederson, P. Singh and X-D.Zhou, *Vacuum*, **80**, 1066 (2006).
8. G. Constantin, C. Rossignol, P. Briois, A. Billard, JP. Barnes, L. Dessemond and E. Djurado, *ECS Transactions*, **45**, 295 (2012).
9. J. A. Thornton, *Journal of Vacuum Science and Technology*, **11**, 666 (1974).
10. A. Anders, *Thin Solid Films*, **518**, 4087 (2010).
11. J. H. Park, S. M. Han, K. J. Yoon, H. Kim, J. Hong, B.-K. Kim, J.-H. Lee and J.-W. Son, *Journal of Power Sources*, **315**, 324 (2016).
12. J. Fondard, P. Bertrand, A. Billard, S. Fourcade, P. Batocchi, F. Mauvy, G. Bertrand and P. Briois, *Solid State Ionics*, **310**, 10 (2017).
13. P. Coddet, M. C. Pera and A. Billard, *Surface and Coating Technology*, **205**, 3987 (2011).
14. J. Fondard, A. Billard, G. Bertrand and P. Briois, *Vacuum*, **152**, 97 (2018).
15. J. Fondard, A. Billard, G. Bertrand and P. Briois, *Solid State Ionics*, **265**, 73 (2014).
16. E. Navickas, M. Gerstl, G. Friedbacher, F. Kubel and J. Fleig, *Solid State Ionics* **211**, 58 (2012).
17. E. Breaz, E. Aubry, A. Billard, N. Coton, P. Coquoz, A. Pappas, S. Diethelm, R. Ihringer, P. Briois, in SOFC-XV, S.C. Singhal and T. Kawada, Editors, PV 78-1, p. 807, *The Electrochemical Society Transactions*, Pennington, NJ (2017).
18. A. Billard and F. Perry, *Technique de l'ingénieur*, **M 1654**.